Spectral Properties of Nonhydrogenic Atoms in Weak External Fields

Thibaut Jonckheere, Benoît Grémaud, and Dominique Delande
Laboratoire Kastler-Brossel, Université Pierre et Marie Curie, Tour 12, Etage 1, 4 Place Jussieu, F-75005 Paris, France
(Received 7 April 1998)

We study how the ionic core in a nonhydrogenic atom modifies the dynamics of a Rydberg electron in the presence of a weak static external field. We show that such a system is neither regular nor chaotic: its energy levels display unusual statistical properties, intermediate between the standard Poisson and random matrix ones. The ionic core acts as a scatterer whose size is comparable to the de Broglie wavelength of the electron, inducing specific quantum effects. [S0031-9007(98)07115-4]

PACS numbers: 32.60.+i, 05.45.+b, 03.65.Sq, 32.80.Rm

The hydrogen atom in the presence of an external magnetic field is a quantum system whose corresponding classical dynamics is either regular or chaotic, depending on the scaled energy $\epsilon = E\gamma^{-2/3}$ (E is the energy and γ is the magnetic field in atomic units), and thus constitutes a prototype for studies on quantum chaos [1].

In correspondence with the evolution of the classical dynamics from quasi-integrable for a weak magnetic field (low negative scaled energy ≤ -0.5) to chaotic at high field (high scaled energy ≥ -0.13), the statistical properties of the energy levels evolve from a Poissonian spectrum to those of the Gaussian orthogonal ensemble (GOE) of random matrices [1]. In the first case, the nearest-neighbor spacing (NNS) distribution—which measures the probability to find the next energy level at distance s (in units of the mean level spacing)—is $P(s) = \exp(-s)$, and, in the second case, it is approximately given by the Wigner distribution $P(s) = \pi s/2 \exp(-\pi s^2/4)$.

In a nonhydrogenic atom—for example, an alkali atom as used in several experiments [2–4]—the Rydberg electron is in a highly excited state while all other electrons are in low excited states. The system (nucleus + inner electrons) can be considered as a frozen ionic core with spherical symmetry, the size of a few Bohr radii. When it is outside this ionic core, the Rydberg electron experiences a Coulomb field created by a charge $Z = 1$ at the nucleus. It is only when it penetrates the core that it feels a stronger force. At the scale of the Rydberg electron (few thousands Bohr radii), the ionic core appears as a very small object perturbing the hydrogenic dynamics.

A nontrivial question—addressed in this Letter—is to determine the spectral properties of a nonhydrogenic atom in an external field. When the classical hydrogenic dynamics is chaotic, it seems that they remain described by the GOE [4]. The situation is totally different when the hydrogenic dynamics is regular because the ionic core breaks the quasi-integrability. Courtney *et al.* [4] have shown a dramatic change in the statistical properties of energy levels which seem to be close to the GOE ones in the presence of the ionic core. They attribute this phenomenon to "core-induced chaos"; we here show that this point of view is incomplete.

An efficient numerical method based on R-matrix theory exists for finding the energy levels of a nonhydrogenic atom in an external field [3]. It relies on the physical picture outlined above: one splits space in an outer region where the effect of the ionic core is negligible and where the Schrödinger equation for the Rydberg electron is solved by expansion on a suitable basis, and an inner region where the quantum dynamics is dominated by the ionic core (the effect of the external field is negligible) and can be described by a set of quantum defects. The matching between the solutions in the two regions gives the energy levels of the nonhydrogenic atom.

We have calculated the lowest 40 000 states of the hydrogen atom in a magnetic field at scaled energy $\epsilon = -0.5$ (for the $L_z = 0$, even parity series) and the same set for the simplest nonhydrogenic atom, imposing a single nonzero quantum defect $\delta_{\ell=0} = 0.5$. This is not too far from a real atom such as lithium where $\delta_0 = 0.4$ and $\delta_{\ell\geq 2} \ll 0.01$. Figure 1 shows the cumulative spacing distribution $N(s) = \int_0^s P(x)\,dx$ obtained for various sequences of energy levels (for $\delta_{\ell=0} = 0.5$), all obtained at the same scaled energy, that is, for the same hydrogenic dynamics. The lowest sequence is well described by the Wigner distribution, but, for higher excited states, the distribution deviates from Wigner and tends to a well defined limit which presents level repulsion—such as the Wigner distribution—at the origin, but also has a much longer tail for large spacings—such as the Poisson distribution [see Figs. 1(d) and (e)]. Clearly, the behavior at large s is exponential, *not* Gaussian. For comparison, we have also plotted the "semi-Poisson" distribution (defined below) [5]:

$$P(s) = 4s\exp(-2s)\,, \tag{1}$$

which is in excellent agreement with our numerical results. We have carefully checked that the numerically obtained distribution does not further change for higher excited states. In other words, when we go to higher and higher Rydberg states at fixed scaled energy, the statistical properties of the energy levels *do not* tend to the ones of the GOE.

A similar phenomenon is observed in an external static electric field. For scaled energy $\epsilon = EF^{-1/2}$ (where F is the electric field in atomic units) sufficiently below the

 0031-9007/98/81(12)/2442(4)$15.00 © 1998 The American Physical Society

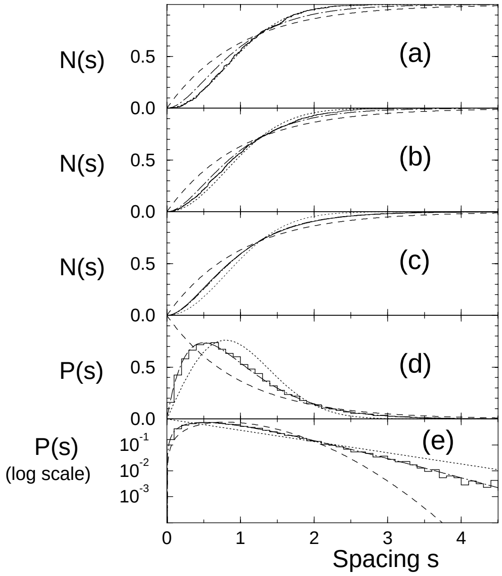

FIG. 1. Statistical properties of the energy levels of a nonhydrogenic atom (quantum defect $\delta_{\ell=0} = 0.5$) in a weak magnetic field (scaled energy -0.5, $L_z = 0$, even parity). (a) Cumulative nearest-neighbor spacing distribution between the 200th and the 700th excited states (solid histogram), compared with the Poisson (dashed line), semi-Poisson (dash-dotted line), and Wigner (dotted line) distributions; (b) and (c) Same as (a), respectively, in the ranges 1000th to 2000th and 5000th to 40 000th excited states; (d) and (e) The nearest-neighbor spacing distribution itself, on linear and logarithmic scales [data as in (c)]. While, for low excited states, the distribution is well described by the Wigner distribution, the distribution for higher excited states is quite different, with a linear level repulsion such as Wigner and an exponential tail such as Poisson. The agreement with the intermediate semi-Poisson distribution is excellent; see especially the tail at large spacing in (e). In the corresponding hydrogenic situation, all of the distributions are close to the Poisson distribution.

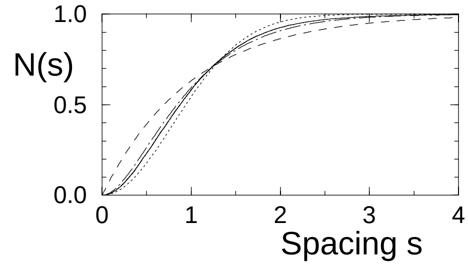

FIG. 2. Same as Fig. 1, but in a weak electric field (scaled energy -2.2) for states ranging from the 20 000th to the 40 000th excited states. Again, the cumulative spacing distribution is clearly different from the Poisson and the Wigner distributions, in good qualitative agreement with the semi-Poisson prediction at small and large s.

classical ionization threshold $\epsilon = -2$, the highly excited states are quasidiscrete. In the absence of an ionic core, the system is integrable and displays a Poisson statistics. For a nonhydrogenic atom, the NNS distribution is linear at small spacing (the cumulative distribution starts as s^2) and falls exponentially at large s—see Fig. 2. Although it slightly deviates from the semi-Poisson distribution (see discussion below), it has the same qualitative behavior at small and large s and is clearly very different from a Wigner distribution. We expect such a behavior to be general for nonhydrogenic atoms in any external field weak enough to keep the classical hydrogenic dynamics quasi-integrable.

A complete understanding requires a careful analysis of the physical phenomena taking place in the vicinity of the ionic core. The crucial point is to know whether a semiclassical approximation may be used there: We argue in the following that the answer is negative and that a specific approach is needed.

The ionic core acts as a spherical obstacle which scatters the Rydberg electron. The size of the scattering object (few Bohr radii) is comparable to the de Broglie wavelength of the Rydberg electron close to the core, even if one considers extremely highly excited states: the ionic core *cannot* be treated as a classical object [6]. The effect of a spherical scatterer is accounted for by a set of phase shifts in the different spherical channels. Here, these phase shifts are nothing but the quantum defects. Different model potentials for the ionic core may give the same set of quantum defects and, consequently, the same spectra in the presence of an external field. They will, however, lead to different classical dynamics [7] and, consequently, to different thresholds for core-induced chaos: this is because near the nucleus, where the core strongly affects the classical trajectories and makes them depend sensitively on the initial conditions, the semiclassical approximation breaks down. It is thus impossible to build a solution of the Schrödinger equation which follows closely one such classical trajectory, the wave packet being unavoidably scattered near the origin [8]. However, the breakdown of the semiclassical approximation is not extremely severe because the de Broglie wavelength is comparable—not much larger—to the size of the ionic core. A semiclassical approximation using core-scattered orbits thus gives a correct qualitative understanding of the physics, for example, the existence of additional modulations in the density of states and density of oscillator strengths [7]. If quantitative results are needed—for example, the amplitudes and phases of these modulations—a quantum *ad hoc* treatment of the ionic core is required, as done in [6]. From a temporal point of view, a typical classical trajectory follows an invariant torus of the hydrogenic motion, being from time to time scattered by the ionic core to another torus. The time interval between two consecutive scattering events is of the order of the Heisenberg time, $\hbar/$(mean level spacing), which expresses that the quantum dynamics can be considered neither as chaotic nor as regular: it is an intermediate situation.

The physics is very similar to the one of a rectangular two-dimensional billiard containing a small circular scatterer, whose size is tuned to the de Broglie wavelength

[9]. While, for a relatively large obstacle, the system (a standard Sinai billiard) has the statistical properties of the GOE, in the limiting case of a point scatterer, these are somewhat different: there is linear level repulsion at small spacing, but the tail significantly deviates from a Gaussian, *exactly* as our numerical observations on nonhydrogenic atoms. Because of particular attention on the level repulsion phenomenon, the distributions obtained in [9] have been incorrectly interpreted as Wigner distributions and thus as proofs of the existence of "wave chaos" of "chaos induced by quantization."

The analogy between a nonhydrogenic atom and such a billiard can be made more formal. Suppose we are able to solve exactly the hydrogenic problem in the presence of an external field. E_i will denote the energy levels and $\psi_i(\mathbf{r})$ the eigenstates. The Green's function is

$$G(E,\mathbf{r},\mathbf{r}') = \sum_i \frac{\psi_i^*(\mathbf{r}')\psi_i(\mathbf{r})}{E - E_i}. \quad (2)$$

At any energy E, $G(E,\mathbf{r},\mathbf{r}')$ (viewed as a function of $\mathbf{r}$) is a solution of the Schrödinger equation for the electron, decreasing at infinity. Moreover, except in the immediate vicinity of the nucleus, it is also a solution of the Schrödinger equation for the nonhydrogenic atom. Hence, the energy spectrum of the nonhydrogenic atom in the presence of the external field is simply given by those values of E for which $G(E,\mathbf{r},\mathbf{r}')$ near $\mathbf{r} = 0$ can be matched with the field-free nonhydrogenic eigenfunctions (which depend on the quantum defects) described in [10]. In the specific case of a single nonzero quantum defect $\delta = \delta_{\ell=0}$, only the $\ell = 0$ spherical component plays a role as the other ones cancel at the origin, and we finally end with the following equation:

$$\sum_i \frac{|\psi_i(\mathbf{0})|^2}{E_i - E} = \frac{\cot(\pi\delta)}{2}, \quad (3)$$

where the sum over i, which is formally divergent, has to be conveniently renormalized. This renormalization process is somewhat tricky and will be explained—together with the general case of several nonzero quantum defects—in detail elsewhere [11]. It is analogous to the one used in [9] for a point scatterer in a billiard (for which a similar equation is obtained for the energy spectrum), taking into account the presence of the Coulomb potential.

Equation (3) not only allows calculation of the nonhydrogenic energy levels as soon as the hydrogenic ones are known, but it also gives much insight in the statistical properties of the energy levels. A first remark is that there is exactly one root between two poles, i.e., one nonhydrogenic energy level in the interval limited by two consecutive hydrogenic levels. We now concentrate on the case $\delta = 0.5$ where the right-hand side (rhs) in Eq. (3) is zero. The statistical properties of the roots of Eq. (3) can be obtained from the statistical properties of the hydrogenic energy levels E_i and the numerators $|\psi_i(\mathbf{0})|^2$. For a quasi-integrable situation, the E_i have a Poisson distribution, but the distribution of the numerators is not universal. It is then easy to show that the NNS distribution of the roots of Eq. (3) decreases similar to $\exp(-2s)$ at large distances (unlike the Wigner distribution) and presents a linear level repulsion $P(s) = \alpha s$ at small s with the coefficient α depending on the distribution of the numerators. When all numerators are equal, one gets $\alpha = \pi\sqrt{3}/2$, significantly smaller than the semi-Poisson prediction $\alpha = 4$, see Eq. (1) [5]. This is the situation realized for a weak external electric field where the eigenstates are separable in parabolic coordinates, and their overlaps with the usual spherical hydrogenic states are given by a Clebsch-Gordan coefficient, which is the same for all states in the case $\ell = m = 0$: the slope near $s = 0$ is smaller than four (see Fig. 2), and a global small deviation from semi-Poisson is observed. For a nonuniform distribution of the numerators, α increases, being for usual smooth distributions close to four, either smaller or larger. This is the case for an external magnetic field where the numerators are widely spread and the global agreement with semi-Poisson almost perfect. In order to understand qualitatively the spectral properties, Bogomolny *et al.* [5] have introduced a simple model—baptized "semi-Poisson model"—for solving approximately Eq. (3), where each zero is lying exactly in the middle of two consecutive poles. The corresponding NNS distribution—called semi-Poisson distribution—is given by Eq. (1) and reproduces well our numerical results (see Figs. 1 and 2).

Several models based on different physical grounds predict linear level repulsion. For example, the "short-range Dyson model" discussed in [5] (where there is level repulsion only between adjacent states, in contrast with

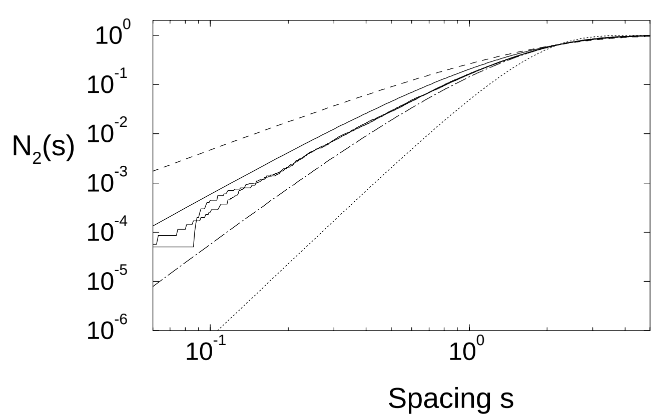

FIG. 3. Cumulative next-nearest-neighbor spacing distributions (on a double logarithmic scale) for a nonhydrogenic atom in a weak magnetic [data of Fig. 1(c)] or electric [data of Fig. 2] field, compared with the Poisson (dashed line), semi-Poisson (solid line), short-range Dyson model (dash-dotted line), and GOE (dotted line) distributions. The functional dependence at small spacing s is clearly proportional to s^3, in agreement with the semi-Poisson model, and deviates from all other distributions.

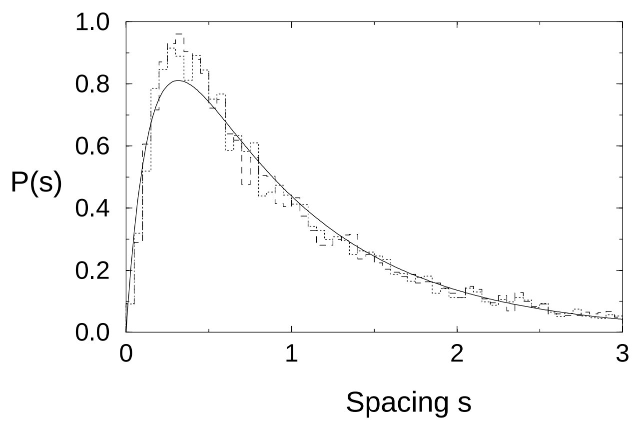

FIG. 4. Spacing distributions for a nonhydrogenic atom in a weak magnetic field (scaled energy −0.5, from 13 000th to 22 000th excited states) with quantum defect $\delta_{\ell=0} = 0.15$ (dotted line) and 0.85 (dashed line) in comparison with the analytical prediction of the δ-Poisson model [Eq. (4)]. The excellent agreement validates the model which smoothly evolves from a Poisson distribution for $\delta = 0$ to a semi-Poisson distribution at $\delta = 0.5$, where the effect of the ionic core is maximum.

the GOE where there is level repulsion between any pair of states) predicts a NNS distribution exactly equal to the semi-Poisson distribution, although other statistical quantities behave differently from the ones of the semi-Poisson model. In order to discriminate between the various models, we study the next-nearest-neighbor distribution $P_2(s)$, i.e., the statistical distribution of spacing between states n and $n+2$. The corresponding cumulative distribution $N_2(s) = \int P_2(x)\,dx$ is shown in Fig. 3 on a double logarithmic scale, in comparison with the predictions of the Poisson, semi-Poisson, short-range Dyson, and GOE models, which behave as s^2, s^3, s^4, and s^5, respectively. Clearly, the numerical results scale as s^3 in good agreement with the semi-Poisson model, in sharp contrast with some other systems displaying intermediate level statistics [5,12], which are closer to the short-range Dyson model. Note that the semi-Poisson model does not predict correctly the coefficient of s^3. Like the NNS, there is no universality here and the model is too crude.

When the quantum defect δ in the $\ell = 0$ channel is not equal to 0.5, the rhs in Eq. (3) is not zero and, in average, the roots are not in the middle of consecutive poles. For equally spaced E_i and equal numerators, Eq. (3) can be exactly solved, and the roots lie exactly at fraction δ of each interval. To describe the general situation (not equally spaced E_i), we define a δ-Poisson model where each level lies at $\delta E_i + (1-\delta)E_{i+1}$. The corresponding spacing distribution is

$$P_\delta(s) = \frac{1}{1-2\delta}\left[\exp\left(-\frac{s}{1-\delta}\right) - \exp\left(-\frac{s}{\delta}\right)\right]. \quad (4)$$

It is shown in Fig. 4 in comparison with the NNS distributions obtained numerically for a nonhydrogenic atom in a magnetic field with $\delta = 0.15$ and 0.85. The agreement is excellent. The same distribution is obtained for quantum defects δ and $1-\delta$, as predicted by Eq. (4).

In conclusion, we have shown that, for a nonhydrogenic atom in a weak external field, the presence of the ionic core which scatters the Rydberg electron leads to statistical properties of the energy levels of a new type, intermediate between the standard Poisson and GOE statistics. Similar observations have been recently reported in other systems [5,12,13], which indicate their importance and broad interest: as far as we know, nonhydrogenic atoms are the first "real" systems where this is numerically observed and where an experimental confirmation could be obtained in the near future.

We thank E. Bogomolny, K. Taylor, and J. Zakrzewski for fruitful discussions. CPU time has been provided by IDRIS. Laboratoire Kastler-Brossel, de l'Ecole Normale Supérieure et de l'Université Pierre et Marie Curie, is unité associée 18 du CNRS.

[1] H. Friedrich and D. Wintgen, Phys. Rep. **183**, 37 (1989); D. Delande, in *Chaos and Quantum Physics*, Proceedings of the Les Houches Summer School, Session LII, edited by M.-J. Giannoni, A. Voros, and J. Zinn-Justin (North-Holland, Amsterdam, 1991).
[2] H. Held, Ph.D. thesis, University of Münich, 1997.
[3] M. H. Halley, D. Delande, and K. T. Taylor, J. Phys. B **26**, 1775 (1993); D. Delande, K. T. Taylor, M. H. Halley, T. Van der Veldt, W. Vassen, and W. Hogervorst, J. Phys. B **27**, 2771 (1994).
[4] M. Courtney and D. Kleppner, Phys. Rev. A **53**, 178 (1996).
[5] E. B. Bogomolny, U. Gerland, and C. Schmit (to be published).
[6] P. A. Dando, T. S. Monteiro, D. Delande, and K. T. Taylor, Phys. Rev. A **54**, 127 (1996); P. A. Dando, T. S. Monteiro, and S. M. Owen, Phys. Rev. Lett. **80**, 2797 (1998).
[7] B. Hüpper, J. Main, and G. Wunner, Phys. Rev. A **53**, 744 (1996).
[8] J. Gao, J. B. Delos, and M. Baruch, Phys. Rev. A **46**, 1449 (1992); J. Gao and J. B. Delos, *ibid.* **46**, 1455 (1992).
[9] P. Seba, Phys. Rev. Lett. **64**, 1855 (1990); T. Shigehara and T. Cheon, Phys. Rev. E **54**, 1321 (1996), and references therein; S. Albeverio *et al.*, *Solvable Models in Quantum Mechanics* (Springer-Verlag, Berlin, 1988); R. L. Weaver and D. Sornette, Phys. Rev. E **52**, 3341 (1995); P. Rosenqvist, N. D. Whelan, and A. Wirzba, J. Phys. A **29**, 5441 (1996).
[10] M. J. Seaton, Rep. Prog. Phys. **46**, 167 (1983).
[11] T. Jonckheere and D. Delande (to be published).
[12] B. Grémaud and S. R. Jain (to be published).
[13] D. Braun, G. Montambaux, and M. Pascaud, Phys. Rev. Lett. **81**, 1062 (1998).